Drastic Au(111) Surface Reconstruction upon Insulin Growth Factor Tripeptide Adsorption

5 AUTHORS, INCLUDING:

Vincent Humblot
Pierre and Marie Curie University - Paris 6
57 PUBLICATIONS **1,336** CITATIONS

Anne Vallée
Université de Versailles Saint-Quentin
15 PUBLICATIONS **286** CITATIONS

Frederik Tielens
Collège de France
93 PUBLICATIONS **1,331** CITATIONS

Claire-Marie Pradier
Pierre and Marie Curie University - Paris 6
**170** PUBLICATIONS **2,831** CITATIONS

Drastic Au(111) Surface Reconstruction upon Insulin Growth Factor Tripeptide Adsorption

Vincent Humblot,* Anne Vallée, Ahmed Naitabdi, Frederik Tielens, and Claire-Marie Pradier

Laboratoire de Réactivité de Surface, UMR CNRS 7197, Université Pierre et Marie Curie—UPMC Paris 6 case 178, 4 place Jussieu, 75005 Paris, France

S *Supporting Information*

ABSTRACT: Adsorption of biomolecules at metal surfaces often creates two-dimensional ordering of the adlayers. However, metal substrate reconstruction is less commonly observed, unless upon annealing of the molecule—surface system. Here, we report on the drastic room-temperature reconstruction of the Au(111) surface, driven by the adsorption of insulin growth factor tripeptide molecules. Scanning tunneling microscopy images show that the surface reconstruction, which takes place without annealing the system, is dynamic and evolves over time. It is initiated at kinks and steps edges, but the reconstruction also takes place within defect-free terraces. Theoretical calculations are performed to explain the reconstruction at the molecular level.
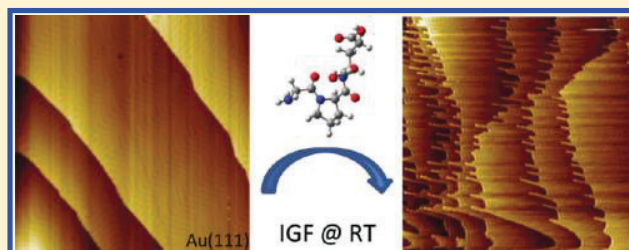
INTRODUCTION

Adsorption of biomolecules on metal surfaces is a relevant topic today, contributing to the understanding of the interface phenomenon in biomaterials, biocompatibility, and chiral recognition.[1] For the past 15 years, adsorption of amino acids on metal surfaces has been studied by means of surface science techniques in combination with quantum chemical calculations, to understand adsorption mode, 2D surface organization, and basic aspects of surface—biomolecule interactions.[2−5]

Adsorption of "bigger" molecules such as C_{60}, or more commonly porphyrins and porphyrin derivatives, under ultra-high-vacuum (UHV) conditions is now often reported.[6,7] However, when dealing with peptides, the challenge is to keep the molecule intact once adsorbed at the metal surface without breaking any molecular bonds due to surface reactivity, for instance. More recently, adsorption of complex biomolecules has been studied on metal surfaces from the liquid phase,[8−11] but peptide adsorption under controlled UHV conditions is yet another challenge.

To our knowledge, only four studies of poly amino acids adsorption under UHV conditions have been reported. In the first one, two homo-tripeptides, tri-L-alanine and tri-L-leucine, were adsorbed onto Cu(110) and studied using reflection—absorption infrared spectroscopy (RAIRS),[12] where the authors confirmed that the molecules are adsorbed intact on the surface. The second and third ones reported the scanning tunneling microscopy (STM) studies of homo-di-L-alanine on Cu(110)[13] and homo-di-L/D-phenylalanine adsorption on Cu(110) and Cu(100).[14,15] In a very recent work, we studied the adsorption on gold and copper surfaces, Au(111), Au(110), and Cu(110), of two hetero-tripeptides, GSH (glu-cys-gly) and insulin growth factor (IGF, gly-pro-glu), by reflection absorption infrared spectroscopy (RAIRS), X-ray photoelectron

spectroscopy (XPS), and low-energy electron diffraction (LEED).[11,16−18]

Here, we report on RAIRS, XPS, and STM analyses of IGF molecules (cf. Figure 1a) adsorbed on Au(111) combined with theoretical calculations. RAIRS and XPS data show that the IGF molecules are intact on the Au(111) surface. Their adsorption induces a strong reconstruction of the Au(111) surface, evidenced by STM imaging with the creation of gold "fingers" at the step edges. Density functional theory (DFT) calculations have demonstrated that the molecules bind mainly via the COO⁻ groups at one end of the molecules and the amino group of the other end, in a chelating form with a gold atom.

RESULTS AND DISCUSSION

The IGF molecules were adsorbed under UHV conditions onto the clean Au(111) surface. From RAIRS and XPS data analyses, we have demonstrated that the IGF molecules are adsorbed intact on the gold surface due to the good correlation with the molecule composition in the XPS data, cf. Supporting Information, and the presence of amide I and II bands in the RAIRS data. In addition, *in situ* RAIRS measurements tell us that the molecules are bound to the gold surface via at least the carboxylate moiety because of the presence of the symmetric stretching COO⁻ signature.

The XPS and PM-RAIRS results highlight the simultaneous presence of COOH, COO⁻, NH_2, and NH_3^+ groups. Like amino acids, IGF exists in a zwitterionic form in the solid state and in neutral form in a gas.[19] We assumed that the molecules of IGF are adsorbed onto gold surfaces under a globally neutral
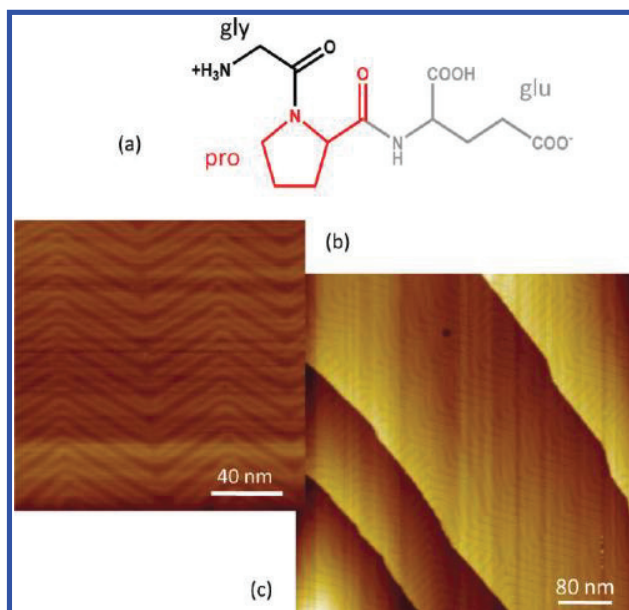
Figure 1. (a) Structure of IGF peptide (gly-pro-glu) in the zwitterionic chemical form. (b,c) STM images of the clean Au(111) surface, 150 nm × 150 nm and 500 nm × 500 nm. Tunneling conditions: U = 0.3 V, I = 200 pA.

Figure 2. Consecutive 500 nm × 500 nm STM images obtained after adsorption of IGF under UHV conditions at room temperature. The images, recorded on the same surface area, show the drastic reconstruction of the surface due to IGF molecules. One terrace is highlighted with dashed lines, showing the evolution of the surface reconstruction. Tunneling conditions: U = 2.0 V, I = 20 pA. The acquisition time runs linearly from (a) to (d), with each image lasting 4 min and 24 s.

form. Two chemical forms have therefore been considered in the present case, the zwitterionic and neutral ones, respectively $NH_3^+/COOH/COO^-$ and $NH_2/COOH/COOH$. The zwitterionic or neutral proportion of IGF can be calculated from the NH_3^+ contribution of the N1s peak with respect to the other N atom contributions, and our calculations show than more than 75% of the IGF tripeptides molecules are present on Au(111) in zwitterionic form.

Figure 1b shows the clean $(22 \times \sqrt{3})$ reconstructed Au(111) surface. On a large-scale STM image, Figure 1c, one can notice the presence of large terraces, from 100 nm up to more than 250 nm wide, without significant defect of the clean surface.

A low coverage of IGF was deposited at room temperature on the clean surface, i.e., $\theta \approx 2$ min of sublimation dose at 2×10^{-9} Torr (base pressure of 1×10^{-10} Torr), and the modified surface was then observed by STM at room temperature. Figure 2 displays consecutive images taken from the same spot area on the surface. One can clearly see that a drastic phenomenon is taking place upon adsorption of tripeptide molecules, with the creation of "fingers" of gold atoms at the step edges, and that the shape and size of the terraces are distinctly modified from one STM image to the next, Figure 2a–d.

This kind of surface reconstruction has already been reported on other metal surface such as copper, for instance. Among the various examples, one can cite the local reconstruction of the Ni(110) surface upon adsorption of tartaric acid, where the local stress, induced by the creation of the chiral footprint of the molecules, is accompanied by the creation of missing and added nickel rows.[20] This local reconstruction takes place at room temperature, but the defects created are only localized around a given molecule, and no displacement of atom over a long distance is observed. However, several studies have reported long-range surface reconstruction on Ag(110), Cu(110), or Pt(110) upon adsorption of organic adsorbates.[21-23]
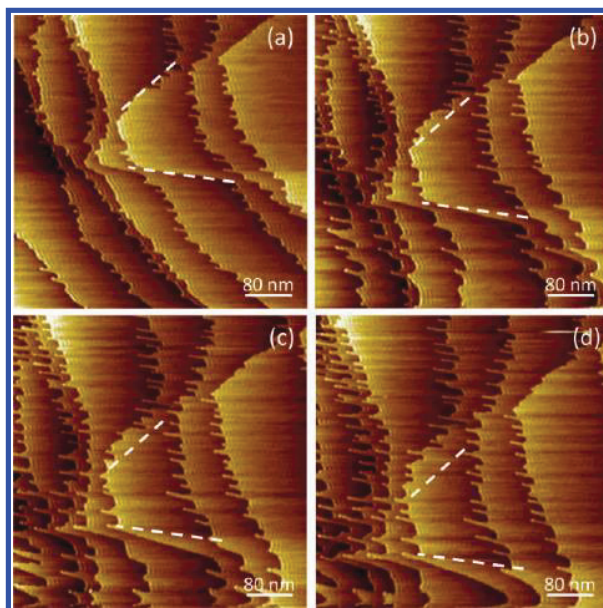
All reported examples involved the presence of carboxylic acid groups that strongly interact with the surface atoms. For instance, Bowker et al.[24] presented the faceting of a Cu(110) surface due to the adsorption of formic acid and a huge mass transportation at kinks and step edges upon annealing. The same phenomenon has been reported upon adsorption of amino benzoic acid on Cu(110) when annealing at 540 K.[25] In all these cases, the authors explained this surface faceting and mass transportation by a strong interaction between the organic molecules and the substrate atoms. In addition, for the reconstruction to occur, annealing is most of the time required, i.e., heat to provide enough energy to overcome the diffusion barrier and enable the molecule–gold atom systems to move. Moreover, these reconstructions are mainly observed on fcc(110) transition metal substrates.

In addition, two other examples of surface reconstruction upon organic material adsorption at room temperature can be found in the literature. Jones et al.[23] reported that glutamic acid molecules, adsorbed at room temperature on Ag(110), also induce a surface faceting at 300 K (a second type of faceting is as well observable when the whole system is heated up to 425 K). The second example is an extensive study on the adsorption of formate on Cu(110) by the group of Leibsle.[26-29] The authors first report the "frizzy" character of the clean Cu(110) surface at room temperature, with atomic diffusion and atom detachment at step edges.[30] When a low coverage of formate is deposited at the surface, this phenomenon carries on, creating triangular structures at the step edges. Eventually, when the coverage is increased up to one saturated monolayer, the adsorbed formate molecules create finger-like islands on a long-range scale.[27] Harrington et al. explained this profound effect of step edges by the increase in the kink density following strong

adsorption of formate, thus enabling the mobility of the whole surface.

Here, most of the required conditions for surface reconstruction and faceting are present: there is a strong interaction between the IGF molecules and the gold substrate, and the coverage is low enough to ensure that the surface is not fully covered by ad-molecules, thus enabling molecule–gold atom clusters to travel across the surface. However, in this case the reconstruction takes place at room temperature (300 K), with no further annealing process, and more importantly, the surface crystallography is fcc(111) and not (110), as reported in the above-cited examples. The "fingers" created upon surface reconstruction are around 10 ± 1 nm wide, their length increasing with time up to 45 ± 2 nm, and they are all running in the same direction. This phenomenon is quite similar to the one observed with the glutamic acid/Ag(110) system, and we think that the process occurring is due to the strong "chelating" interactions between the COOH and NH$_2$ groups with the gold.

The process driving this drastic gold reconstruction upon IGF adsorption remains unclear. The strong interactions taking place between the molecules and the gold atoms from the first layer will probably weaken the crystal cohesion forces of the topmost layers. Thus, under the tunneling conditions of the STM experiments, the tip-induced electrostatic field affects the stability of the surface atoms. The observed mass transportation is not, strictly speaking, "mechanically driven" by the STM tip–surface interaction, but rather due to an energetically favorable process for the molecules–gold atoms system mobility. This hypothesis is reinforced by the extremely mild tunneling conditions applied, 2 V and 20 pA; the distance tip–surface is then greater than those usually used for manual and mechanical atom removal or displacement, where the tunneling current is usually 100 times higher than the current used for normal imaging.[30−32]

In order to support our hypothesis, quantum chemical calculations were performed using periodic DFT by means of the program VASP.[33,34] A model was built to explain the origin of the "finger" formation phenomenon on the gold surface by comparing the results with DFT calculations performed on the geometrically related molecule methionine. It is known that methionine does not provoke this type of reconstruction on Au(111) surfaces,[35] probably due to the weak interaction of methionine molecules with the gold surface.

After a series of test calculations for building a pertinent model, as discussed in the Supporting Information, we ended up with the adsorption of IGF on Au(110) surface, taken as a model of a surface step edges or, even better, a surface with under-coordinated atoms.

It was found that the IGF molecule adsorbs strongly in its neutral non-zwitterionic form on a Au$_2$ gas-phase cluster (Figure 3). Using a Au(110) surface showing a row of under-coordinated gold atoms, one could represent the adsorption geometry of IGF on one of the "fingers" observed experimentally.

On the (111) surface the IGF molecule adsorption is weaker; it may adsorb in a geometry similar to that observed for the Au$_2$ cluster, but stabilizing both end groups implicated in the chelating with an intramolecular hydrogen bond (see Figure 4). Calculations show that this H-bond induces a proton transfer, forming COO$^-$ and NH$_3^+$, zwitterionic groups, in line with the experimental observations.
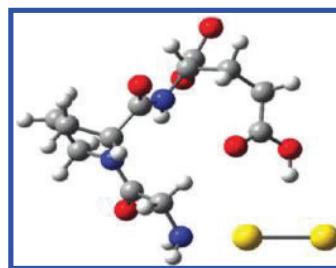

Figure 3. Most stable IGF-Au$_2$ geometry showing the chelating effect of the NH$_2$ and COOH groups.
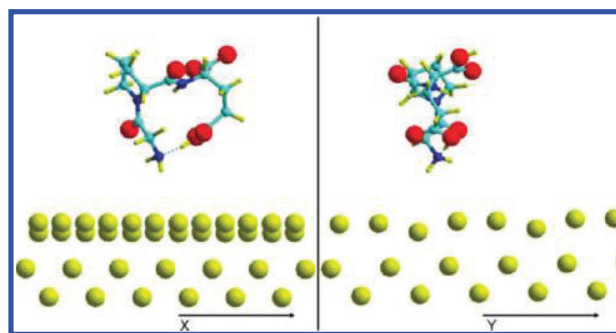

Figure 4. Optimized IGF molecule adsorbed on the Au(110) surface (XZ and YZ view), showing the intramolecular H-bond between the NH$_2$ and COOH zwitterionic precursor groups and the adsorption via those groups.

The comparison calculations with methionine confirm the much stronger adsorption of IGF. It is interesting to note that, although methionine adsorbs via the same terminal groups in its zwitterionic form, IGF adsorbs with an energy of −3.79 eV, which is 2.31 eV higher than for methionine. This difference can be explained partly by the higher dipole moment and higher conformational flexibility of IGF. It is expected, on the basis of reaction energetics, that these 2.31 eV of extra interaction energy are responsible for the surface reconstruction. Thus, if this energy exceeds the cohesion energy and the reaction energy barrier associated with the displacement of gold atoms,[36] surface reconstruction is favored, thus explaining the observed "finger" formation.

In order to understand how the finger creation takes place, we performed low-temperature STM experiments. The mass transportation was initiated at room temperature after deposition of IGF as previously explained, and the system was then cooled to 10 K for imaging. Figure 5 presents STM images acquired under different tunneling conditions to reveal either the reconstructed surface or the molecules. On a large scale, Figure 5A, one can notice the creation of fingers on the edge of a large terrace. By looking in greater details, Figure 5B, the fingers appear to have similar shape and size, roughly 20–25 nm long and 5–7 nm wide, with some random defects. Figure 5D presents the same scanned area, but the tunneling conditions were changed in order to visualize now the IGF molecules. One can see that most of the tripeptide aggregates are located on top of the fingers up to the very beginning of the finger on the terrace. There are not many adsorbed molecules on the terraces at that stage. This clearly confirms that the fingers are a mixed molecule–metal structure.

Finally, Figure 5C provides further evidence of the mass transportation that occurs following adsorption of IGF and finger creation. In Figure 1, one can notice that the herringbone
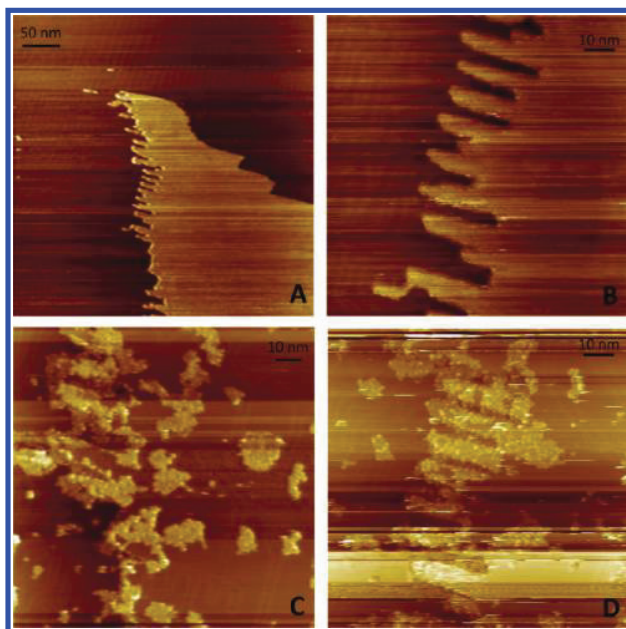
Figure 5. STM images obtained after adsorption of IGF under UHV conditions at low temperature (10 K). The images, recorded under different tunneling conditions, show only the Au(111) surface with the creation of gold fingers in (A) and (B), and the IGF molecules in (C) and (D). STM images conditions: (A) 400 nm × 400 nm, $U = 0.3$ V, $I = 50$ pA; (B) 100 nm × 100 nm, $U = -1.0$ V, $I = 30$ pA; (C) 115 nm × 115 nm, $U = -2.5$ V, $I = 30$ pA; (D) 100 nm × 100 nm, $U = -2.5$ V, $I = 20$ pA.

reconstruction is running symmetrically and unaltered over the whole terrace, with some negligible defect at the elbow of the reconstruction. In contrast, in Figure 5C, the herringbone reconstruction visible on both up and down terraces besides the IGF molecules is now quite altered. This is a sign of a huge relaxation of the constrained $(22 \times \sqrt{3})$ original Au(111) surface, due to the mass transportation and the resulting "growth " of gold fingers of a given higher terrace on top on the lower one.

Figure 6 displays STM images of the IGF/Au(111) surface recorded in the middle of a large terrace after a slight increase of the surface coverage. These results show, for the first time, that the peptide−gold interactions are so strong that mass transportation can occur not only at kinks and step edges, but also on more compact areas such as terraces, without following
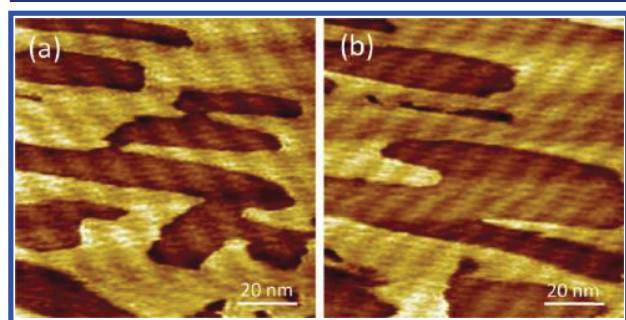

Figure 6. Successive STM images of the Au(111) surface, acquired on the same area, after 2 min adsorption of IGF at room temperature, showing terraces under reconstruction; 100 nm × 100 nm. Tunneling conditions: $U = 2.0$ V, $I = 20$ pA.

preferential crystallographic directions as often observed for fcc(110) surfaces.

CONCLUSION

Combining *in situ* XPS, RAIRS, and STM experiments with *ab initio* DFT calculations gives a unique set of data which enables the interpretation of the surprising behavior of IGF adsorbed on Au(111). We have shown that IGF tripeptide molecules are adsorbed intact on a Au(111) surface. The molecules are present mainly as zwitterionic chemical forms, with a small fraction of neutral molecules, with a ratio of ∼75:25.

Based on experimental RAIRS and XPS results, the adsorption model via both ends of the molecules (NH_3^+ and COO^-) was confirmed as the most stable geometry by DFT calculations. The molecule−surface interaction has been calculated to be 2.5 times higher than usually observed for simple adsorption of an amino acid in the same chemical form on Au(111) under the same conditions. In fact, the IGF molecule's adsorption energy is so high that its interaction with a gold atom is stronger than the cohesion energy between the surface gold atoms.

The IGF−gold atom clusters are thus very mobile on the surface, and these reconstructions take place at *room temperature*, without need for a further annealing, at step edges and inside defect-free terraces, and they are dynamic over time, as shown by successive recorded STM images.

ASSOCIATED CONTENT

ⓢ Supporting Information
Materials, PM-RAIRS, XPS, and STM setup, experimental details; procedure, DFT methodology, and relaxation geometry optimization, Figures S1−S5 and Tables S1−S3. This material is available free of charge via the Internet http://pubs.acs.org.

AUTHOR INFORMATION

Corresponding Author
vincent.humblot@upmc.fr
Notes
The authors declare no competing financial interest.

ACKNOWLEDGMENTS

REFERENCES

(1) Kasemo, B. *Surf. Sci.* **2002**, *500*, 656−677.
(2) Barlow, S. M.; Raval, R. *Surf. Sci. Rep.* **2003**, *50*, 201−341.
(3) Ihs, A.; Liedberg, B.; Uvdal, K.; Törnkvist, C.; Bodö, P.; Lundström, I. *J. Colloid Interface Sci.* **1990**, *140*, 192−206.

(4) Smerieri, M.; Vattuone, L.; Costa, D.; Tielens, F.; Savio, L. *Langmuir* **2010**, *26*, 7208−7215.

(5) Tielens, F.; Humblot, V.; Pradier, C.-M. *Surf. Sci.* **2008**, *602*, 1032−1039.

(6) Donovan, P.; Robin, A.; Dyer, M. S.; Persson, M.; Raval, R. *Chem.−Eur. J.* **2010**, *16*, 11641−11652.

(7) Dyer, M. S.; Robin, A.; Haq, S.; Raval, R.; Persson, M.; Klimes, J. *ACS Nano* **2011**, *5*, 1831−1838.

(8) Feyer, V.; Plekan, O.; Tsud, N.; Chab, V.; Matolin, V.; Prince, K. C. *Langmuir* **2010**, *26*, 8606−8613.

(9) Iucci, G.; Battocchio, C.; Dettin, M.; Gambaretto, R.; Di Bello, C.; Borgatti, F.; Carravetta, V.; Monti, S.; Polzonetti, G. *Surf. Sci.* **2007**, *601*, 3843−3849.

(10) Törnkvist, C.; Liedberg, B.; Lundström, I. *Langmuir* **1991**, *7*, 479−485.

(11) Vallée, A.; Humblot, V.; Méthivier, C.; Pradier, C.-M. *Surf. Interface Anal.* **2008**, *40*, 395−399.

(12) Barlow, S. M.; Haq, S.; Raval, R. *Langmuir* **2001**, *17*, 3292−3300.

(13) Stensgaard, I. *Surf. Sci.* **2003**, *545*, L747−L752.

(14) Lingenfelder, M.; Tomba, G.; Costantini, G.; Ciacchi, L. C.; De Vita, A.; Kern, K. *Angew. Chem., Int. Ed.* **2007**, *46*, 4492−4495.

(15) Wang, Y.; Lingenfelder, M.; Classen, T.; Costantini, G.; Kern, K. *J. Am. Chem. Soc.* **2007**, *129*, 15742−15743.

(16) Méthivier, C.; Lebec, V.; Landoulsi, J.; Pradier, C.-M. *J. Phys. Chem. C* **2011**, *115*, 4041−4046.

(17) Vallée, A.; Humblot, V.; Méthivier, C.; Pradier, C.-M. *Surf. Sci.* **2008**, *602*, 2256−2263.

(18) Vallée, A.; Humblot, V.; Méthivier, C.; Pradier, C. M. *J. Phys. Chem. C* **2009**, *113*, 9336−9344.

(19) Shin, T.; Kim, K.-N.; Lee, C.-W.; Shin, S. K.; Kang, H. *J. Phys. Chem. B* **2003**, *107*, 11674−11681.

(20) Humblot, V.; Haq, S.; Muryn, C.; Hofer, W. A.; Raval, R. *J. Am. Chem. Soc.* **2001**, *124*, 503−510.

(21) Chen, Q.; Richardson, N. V. *Prog. Surf. Sci.* **2003**, *73*, 59−77.

(22) Gritsch, T.; Coulman, D.; Behm, R. J.; Ertl, G. *Surf. Sci.* **1991**, *257*, 297−306.

(23) Jones, T. E.; Baddeley, C. J.; Gerbi, A.; Savio, L.; Rocca, M.; Vattuone, L. *Langmuir* **2005**, *21*, 9468−9475.

(24) Bowker, M.; Poulston, S.; Stone, P. *J. Phys.: Condensed Matter* **1998**, *10*, 7713.

(25) Chen, Q.; Frankel, D. J.; Richardson, N. V. *Langmuir* **2001**, *17*, 8276−8280.

(26) Haq, S.; Leibsle, F. M. *Surf. Sci.* **1997**, *375*, 81−90.

(27) Harrington, S. J.; Kilway, K. V.; Zhu, D. M.; Phillips, J. M.; Leibsle, F. M. *Surf. Sci.* **2006**, *600*, 1193−1200.

(28) Leibsle, F. M.; Haq, S.; Frederick, B. G.; Bowker, M.; Richardson, N. V. *Surf. Sci.* **1995**, *343*, L1175−L1181.

(29) Silva, S. L.; Patel, A. A.; Pham, T. M.; Leibsle, F. M. *Surf. Sci.* **1999**, *441*, 351−365.

(30) Eigler, D. M.; Lutz, C. P.; Rudge, W. E. *Nature* **1991**, *352*, 600−603.

(31) Eigler, D. M.; Schweizer, E. K. *Nature* **1990**, *344*, 524−526.

(32) Meyer, G.; Bartels, L.; Rieder, K.-H. *Comput. Mater. Sci.* **2001**, *20*, 443−450.

(33) Kresse, G.; Furthmuller, J. *Phys. Rev. B* **1996**, *54*, 11169.

(34) Kresse, G.; Joubert, J. *Phys. Rev. B* **1999**, *59*, 1758.

(35) Naitabdi, A.; Humblot, V. *Appl. Phys. Lett.* **2010**, *97*, 223112.

(36) Swart, J. C. W.; van Helden, P.; van Steen, E. *J. Phys. Chem. C* **2007**, *111*, 4998−5005.